This is an open access article published under an ACS AuthorChoice License, which permits copying and redistribution of the article or any adaptations for non-commercial purposes.

Inorganic Chemistry

Article

pubs.acs.org/IC

Syntheses of Two Vanadium Oxide–Fluoride Materials That Differ in Phase Matchability

Martin D. Donakowski,[†] Romain Gautier,[†] Hongcheng Lu,[†,‡] T. Thao Tran,[§] Jacqueline R. Cantwell,[†] P. Shiv Halasyamani,[§] and Kenneth R. Poeppelmeier*[,†]

[†]Department of Chemistry, Northwestern University, 2145 Sheridan Road, Evanston, Illinois 60208-3113, United States

[‡]State Key Laboratory of Solidification Processing, School of Materials Science and Engineering, Northwestern Polytechnical University, 127 Youyixilu Road, Xi'an 710072, China

[§]Department of Chemistry, University of Houston, 112 Fleming Building, Houston, Texas 77204, United States

Supporting Information

ABSTRACT: The syntheses of two noncentrosymmetric (NCS) vanadium oxide–fluoride compounds that originate from the same synthetic reagent concentrations are presented. Hydrothermal and low-temperature syntheses allow the isolation of metastable products that may form new phases (or decompose) upon heating and allow creation of chemically similar but structurally different materials. NCS materials synthesis has been a long-standing goal in inorganic chemistry: in this article, we compare two chemically similar NCS inorganic materials, $NaVOF_4(H_2O)$ (**I**) and $NaVO_{2-x}F_{2+x}$ (**II**; $x = {}^1/_3$). These materials originate from the same, identical reagent mixtures but are synthesized at different temperatures: 100 °C and 150 °C, respectively. Compound **I** crystallizes in $Pna2_1$: a = 9.9595(4) Å, b = 9.4423(3) Å, and c = 4.8186(2) Å. Compound **II** crystallizes in $P2_1$: a = 6.3742(3) Å, b = 3.5963(2) Å, c = 14.3641(7) Å, and β = 110.787(3)°. Both materials display second-harmonic-generation activity; however, compound **I** is type 1 non-phase-matchable, whereas compound **II** is type 1 phase-matchable.

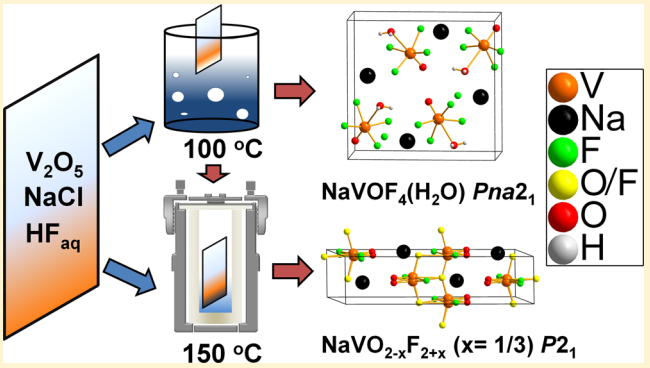

INTRODUCTION

This paper presents two materials that originate from the same synthetic reagents but differ in second-harmonic-generation (SHG) phase matchability. Materials for SHG applications require a noncentrosymmetric (NCS) arrangement of their crystal structure.[1−4] These compounds are often characterized by acentric basic building units (BBUs) such as polar early-transition-metal (ETM) polyhedra or lone-pair cations;[5−10] the synthesis of NCS materials is an ongoing challenge with contributions toward SHG-active materials, piezoelectrics, multiferroics, and other functional solids.[11,12] As per Chen's Anionic Group theory, to design efficient SHG-active crystals, not only should the BBUs display strong individual polar moments, but also the polar moments should be aligned along one direction (specifically along one crystallographic axis).[13] These conditions are achieved in the technologically useful $LiNbO_3$ and $KTiOPO_4$ materials.[14]

Various works have described the use of polar anions with different polyhedral geometries to construct polar solids.[6,15−19] We, and others, have described the use of multiple ions (such as an octahedral ion and a tetrahedral ion) to generate polar materials because the disparate ions would not be relatable via symmetry operations.[15,17−20] In the materials of $Rb_5Nb_3OF_{18}$ (ions of $[NbF_7]^{2-}$ and $[NbO_{2/2}F_4]$)[15,17] and $Ag_3(MoO_3F_3)(MoO_4)Cl$ (ions of $[MoO_3F_3]^{3-}$ and $[MoO_4]^{2-}$),[16] the crystal structures show polar alignment of $[MoO_3F_3]^{3-}/[MoO_4]$ or $[NbO_{2/2}F_4]$ ions. The vanadate family of compounds offers interesting properties of recorded NCS arrangements, multiple ionic environments (strong polar distortions that exist in both tetrahedral and octahedral arrangements),[21] and magnetic activity of vanadium(3+/4+) ions that can contribute to the possibility of multiferroics.[22]

We have made attempts to synthesize oxide–fluoride vanadates with mixed ionic content because vanadium cations can exist as $[VO_4]^{3-}$ tetrahedra and $[VO_xF_{6-x}]^{n-}$ octahedra.[9,23,24] In this manner, a mixed-valence vanadium(4+/5+) material could have isolated $[V^{5+}O_4]^{3-}$ tetrahedra and $[V^{3+/4+}O_xF_{6-x}]^{n-}$ octahedra. Hydrochloric acid is a known reducing agent of vanadium;[25,26] an in situ reduction process would create vanadium(4+), while vanadium(5+) would also be present under nonequilibrium conditions. This process produced the fully vanadium(4+) NCS $CuVOF_4(H_2O)_7$.[9] More recently, we employed bromide ions of KBr in acidic

Special Issue: To Honor the Memory of Prof. John D. Corbett

Received: June 21, 2014
Published: August 19, 2014

 © 2014 American Chemical Society dx.doi.org/10.1021/ic501486x | Inorg. Chem. 2015, 54, 765−772

hydrothermal conditions to reduce vanadium(5+) to form the fully vanadium(4+) $KV^{4+}OF_3$.[27]

Sodium chloride was then examined as a reducing agent of V_2O_5. The reaction of sodium chloride in hydrofluoric acid with vanadium oxide produces two products in similar synthetic conditions: $NaVOF_4(H_2O)$ (**I**) and $NaVO_{2-x}F_{2+x}$ (**II**), where $x = {}^1/_3$. Notably, the structures are both NCS: compound **I** is type 1 non-phase-matchable (NPM), while compound **II** is type 1 phase-matchable (PM). Analyses of similar synthetic conditions could afford similar NCS materials that allow for a better understanding of tailoring phase matchability in solid-state, purely inorganic materials.

EXPERIMENTAL METHODS

Caution! *Hydrofluoric acid is toxic and corrosive! It must be handled with extreme caution and the appropriate protective gear and training.*[28−30] *The dissolution of compounds in aqueous hydrofluoric acid can be exothermic and may cause volatilization of hydrofluoric acid. The use of Teflon at elevated temperatures allows HF_{aq} to permeate the film; caution should be used in handling the backfill of hydrothermal reactions. Vanadium oxide has noted toxicity, particularly when in small, particulate form; vanadium oxide should be handled cautiously and in well-ventilated areas.*[31]

Materials. Hydrofluoric acid (49% HF in water by weight) was obtained from Sigma-Aldrich. Vanadium oxide (V_2O_5, 99.6% min) and sodium chloride (NaCl, 99%) were obtained from Alfa-Aesar. Deionized water was used as backfill in the pressure vessel and as boiling water. All reagents were used as received.

Synthesis. The compound $NaVOF_4(H_2O)$ (**I**) was synthesized by combining 0.5475 g of V_2O_5 (6.020 mmol V^{5+}), 0.3514 g of NaCl (6.013 mmol Na^+), and 1.00 mL of HF_{aq} (24.5 mmol HF) in a Teflon pouch that was made and sealed as previously described.[32−34] The pouch was then placed in a beaker of boiling water, and the reaction mixture was refluxed within the pouch for 30 min. The pouch was removed and immediately allowed to cool. The contents were allowed to crystallize for an additional 48 h, and the pouch was opened and filtered in air to afford a mixture of clear platelets of **I** and NaCl. The pH of the reaction mixture was about 1 before and after the reaction. To monitor reaction conditions, two reactions with identical contents were performed simultaneously with the reaction described above, but the contents were removed after reaction for total periods of 1 and 2 h. Powder X-ray diffraction (PXRD) scans showed the presence of NaCl in the remaining product mixtures. We were unable to avoid the presence of NaCl either by alteration of the reaction conditions or by rinsing with water after the synthesis because **I** is water-soluble.

The compound $NaVO_{2-x}F_{2+x}$ (**II**; $x = {}^1/_3$) was synthesized by the combination of the same amounts of reagents as those for **I** [0.5330 g of V_2O_5 (5.861 mmol V^{5+}), 0.3520 g of NaCl (6.023 mmol Na^+), and 1.00 mL of HF_{aq} (24.5 mmol HF)] in a Teflon pouch, but the pouch was placed in a Parr acid digestion vessel, individually, heated to 150 °C, held at that temperature for 24 h, cooled at a rate of 0.1 °C/min, removed, allowed to sit at ambient conditions for 48 h, filtered in air, rinsed with deionized water three times to remove unreacted NaCl, and allowed to dry to obtain 0.3441 g of clear, dark-blue platelets of compound **II** (2.374 mmol, 40.51% yield with respect to V_2O_5). It was found that if a pouch of **I** (before the pouch was opened) was subsequently placed in the hydrothermal conditions described above, compound **II** was formed. PXRD scans with laboratory radiation did not show other phases in the obtained compound **II**; see the Supporting Information (SI).

Inductively Coupled Plasma Atomic Emission Spectroscopy (ICP-AES). Compound **I** was unable to be examined for elemental content because we were unable to obtain the compound phase-pure. To confirm the metallic content of **II**, ICP-AES was performed. Standard solutions were prepared with Millipore-filtered water with a solution of 997 μg/mL vanadium in 1.3% nitric acid in water (Ricca) and a solution of 1000 μg/mL sodium in 2% nitric acid in water (Fluka). Three samples of **II** were dissolved in 10 mL of nitric acid, separately, and diluted to the appropriate concentrations with Millipore-filtered water. The concentrations of the three separate samples were averaged. The spectra were acquired and analyzed with Varian *ICP-expert II* software. The concentrations of vanadium and sodium for each sample were obtained with the spectral emission peak of the ICP-AES spectrum that was the most Gaussian in shape. Each concentration was obtained by the average of five measurements on the same sample. The results showed a 1:1.000(54) ratio of elemental vanadium/sodium.

Fluoride Elemental Analysis. A sample of compound **II** was examined via ion-selective-electrode analysis by Midwest Microlab, LLC. The analysis was performed on three separate samples to reveal an elemental content of 30.88(23)% by mass. This corresponds to a formula of $NaVO_{2-x}F_{2+x}$ [x = 0.3234(167)] or approximately $Na(V^{4+}V^{5+}_2)_xO_{2-x}F_{2+x}$ ($x = {}^1/_3$). This material shows increased fluoride content compared to the previously published material $NaVO_2F_2$ and results in mixed oxide−fluoride occupancy on crystallographic sites of the structure. The fluoride content increased as a result of charge balance to account for vanadium(4+) that was observed via magnetic susceptibility.

Single-Crystal X-ray Crystallography. Single crystals of compounds **I** and **II** were mounted on a glass fiber in paratone oil and cooled to 100 K under a flow of nitrogen. The data were obtained with a Bruker Kappa APEX 2 CCD diffractometer using monochromated Mo Kα radiation (λ = 0.71073 Å). The crystal-to-detector distance was 60 mm. The data were integrated with the use of the *SAINT-V7.23A* program.[35] Absorption corrections (multiscan, *SADABS*) were applied to the data in the program *APEX2*.[36] The structures were solved with the use of XS to determine the atomic coordinates of the metallic cations;[37] the resulting anions and parameters were refined with Fourier difference maps with the *ShelXL* algorithm within the *Olex2* suite.[37,38] The unit cell of **II** is a commensurate modulation of a previous structure, $NaVO_2F_2$.[39,40] The satellite peaks that arise from this modulation are shown in the SI. Full crystallographic data sets were obtained on the same crystal at 100 and 298 K, and the **q** vector was invariant; this indicates a commensurate modulation, and thus a supercell was used to describe the system.

The unit cell and space group of **II** was ambiguous: the structure could be described in six different unit cell/space group combinations. The structure could additionally be described in two centrosymmetric (CS) settings, but these were disregarded because the material exhibited an SHG response (characteristic of NCS structures) and poor refinement parameters (see the SI). The structure was solved in each possibility with the same weighting scheme, and significant disorder was present in **II** as a result of valence disorder [disorder of vanadium(4+)/vanadium(5+) on the same site]. Under single-crystal X-ray crystallography, it was determined that the vanadium cations were split along bonds to specific anions X (X = O, F); this indicates disorder of the X site. The crystal was solved in each of six possible descriptions, and Hamilton's *R* test was applied to determine the best description.[41] The model that showed the greatest correspondence to the data, as determined from the *R* factors, was used to describe the crystal. The crystallographic parameters for this model are provided in Table 1. The CIFs for compounds **I** and **II** are provided in the SI.

A summary of the other unit cell/space group descriptions and refinement is provided in the SI. The obtained crystal structure of compound **II** is a model of the obtained data: further investigation into the disorder may show long-range order of the oxide−fluoride moieties that lie along 1D chains. The elemental occupancies at these sites were defined with the data acquired from elemental analyses to arrive at the formula of **II**. Refinement of the commensurate structure with the subcell and **q** vector (0, 0, ${}^1/_2$) in the program *JANA2006* showed that the vanadium positional disorder was present if the commensurate symmetry was accounted for; subsequently, the supercell was used for further analysis for simplicity. Symmetry analysis with *PLATON* suggested halving of the unit cell of **II** with maintenance of the space group (e.g., returning to the unit cell of $NaVO_2F_2$), but this was disregarded owing to the satellite peaks observed. *PLATON* showed no additional symmetry beyond this for **I** or **II**.[42]

dx.doi.org/10.1021/ic501486x | *Inorg. Chem.* 2015, 54, 765−772

Table 1. Crystal Data and Refinement for Compounds I and II

	I	II
empirical formula	$F_4H_2NaO_2V$	$F_{4.67}Na_2O_{3.34}V_2$
fw	183.95	289.86
temperature (K)	100.03	100.05
wavelength (Å)	0.71073	0.71073
cryst syst	orthorhombic	monoclinic
space group	$Pna2_1$ (No. 33)	$P2_1$ (No. 4)
unit cell dimens		
a (Å)	9.9595(4)	6.3742(3)
b (Å)	9.4423(3)	3.5963(2)
c (Å)	4.8186(2)	14.3641(7)
β (deg)		110.787(3)
volume (Å^3)	453.14(3)	307.84(3)
Z	4	2
density (calcd) (g/cm^3)	2.696	3.127
abs coeff μ (mm^{-1})	2.285	3.236
F(000)	352	273.3
cryst size (mm^3)	0.21 × 0.09 × 0.04	0.056 × 0.03 × 0.03
θ range for data	2.97−31.50°	3.21−43.10°
index ranges	$-14 \le h \le 14$, $-13 \le k \le 13$, $-7 \le l \le 7$	$-12 \le h \le 12$, $-6 \le k \le 2$, $-27 \le l \le 27$
reflns collected	17392	10434
indep reflns	1511 [R_{int} = 0.0240]	2843 [R_{int} = 0.0543]
completeness to θ	100%, θ = 31.51°	99.7%, θ = 43.10°
refinement method	full-matrix least squares on F^2	full-matrix least squares on F^2
data/restraints/ param	1511/1/81	2843/1/128
goodness-of-fit	1.160	1.011
Flack parameter	0.039(7)	0.03(3)
final R indices [$I > 2\sigma(I)$]	R_{obs} = 0.0117, wR_{obs} = 0.0326	R_{obs} = 0.0331, wR_{obs} = 0.0859
R indices (all data)	R_{all} = 0.0121, wR_{all} = 0.0329	R_{all} = 0.0530, wR_{all} = 0.1014
extinction coeff	none	0.014(3)
largest diff peak and hole (e/Å^3)	0.216 and −0.378	0.733 and −0.890

SHG Measurements. Samples of **I** and **II** were ground with a mortar and pestle and sieved into discrete size ranges. Synthesis of **I** resulted in unreacted NaCl that could not be avoided or separated from **I**. The presence of NaCl dilutes the SHG-active phase. The SHG response was measured with the Kurtz−Perry method and compared to standards of α-SiO_2.[2,43] The results are presented in Figure 1. The average nonlinear-optical susceptibilities of **I** and **II** are approximately 0.55 and 1.15 pm/V, respectively. Compound **I** is NPM, while **II** is PM.

Magnetic Susceptibility. A 57.0 mg polycrystalline sample of **II** was placed in a polyethylene bag. The sample was placed in a Magnetic Property Measurement System (MPMS)-XL magnetometer from Quantum Design. The sample was measured under a 1000 Oe field in a zero-field-cooled (ZFC) scan, a 5000 Oe field in ZFC and field-cooled scans, and a 1 T field in a ZFC scan. The resulting magnetic susceptibilities were corrected for the diamagnetic contributions of polyethylene ($50/\pi \times 10^{-8}$ emu/kg) and the diamagnetism of the compound (-53.033×10^{-6} emu/mol). The spectra showed temperature-independent paramagnetism, and a term was included to account for this phenomenon. The resulting fits showed μ_{eff} of 0.303 μ_B/mol, which is consistent with a material with $\sim^1/_3$ vanadium(4+) present per mole.

Fourier Transform Infrared (FTIR) Spectroscopy. The FTIR spectra of **I** and **II** were obtained on a Bruker 37 Tensor FTIR instrument equipped with an ATR accessory with a germanium crystal. The spectra were obtained from 550−4000 cm^{-1} with 256 scans at 2 cm^{-1} resolution, and a background spectrum was subtracted. The data of the V−X stretching region for compound **II** (550−1200 cm^{-1}) was then fit to a summation of Gaussian functions. The resulting spectra and fitting parameters are provided in the SI. For compound **II**, no absorptions that could be attributed to X−H (X = F^-, O^{2-}) stretches are observed, which indicates that no protons are present within the structure. Compound **I** contained impurities so its FTIR spectrum was not fit, but the spectrum displays a broad peak that corresponds to water moieties present in the compound.

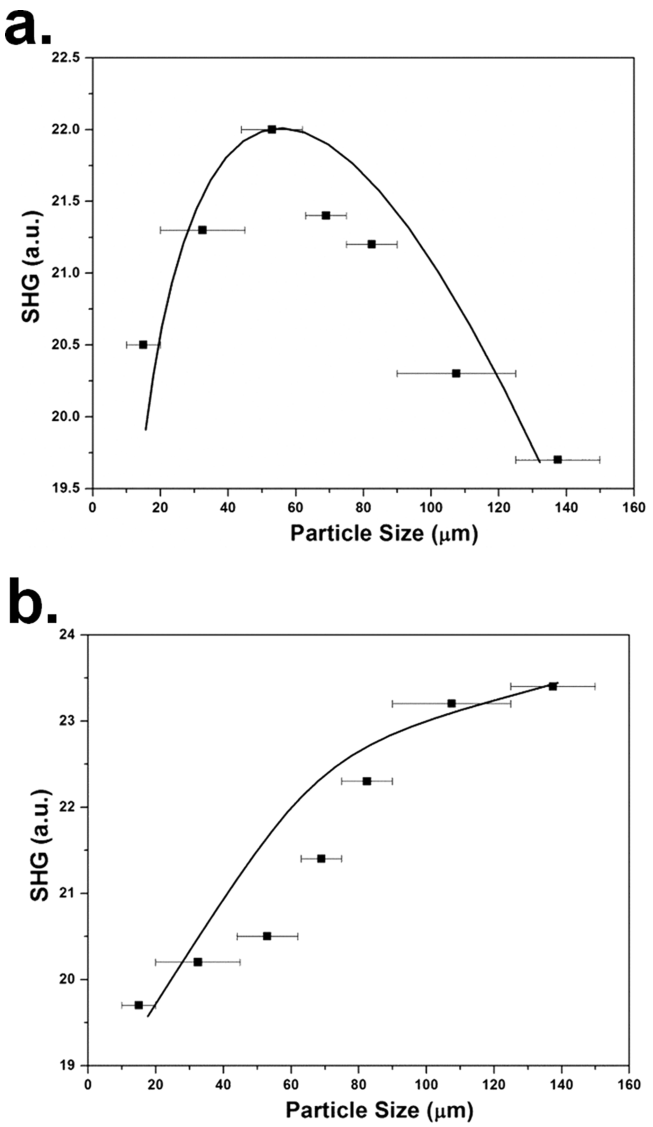

Figure 1. SHG responses as a function of the particle sizes for (a) compound **I** (type 1 NPM) and (b) compound **II** (type 1 PM). The lines are drawn to guide the eye and are not fits to the data.

RESULTS

Structural Descriptions. Despite identical initial reagents, **I** and **II** exhibit vastly different structures. The BBUs of **I** are shown in Figure 2a. The structure contains 0D BBUs of $[VOF_4(H_2O)]^-$ anions that are separated from other vanadium moieties. The sodium cations exist in octahedra with fluoride anions and a coordinated water molecule. The octahedral environments of these species are shown in Figure 2b: the vanadium octahedron coordinates solely to the sodium cations via fluoride anions and the water molecule; the oxide anion coordinates solely to the vanadium ion to fulfill its valence. The

dx.doi.org/10.1021/ic501486x | Inorg. Chem. 2015, 54, 765−772

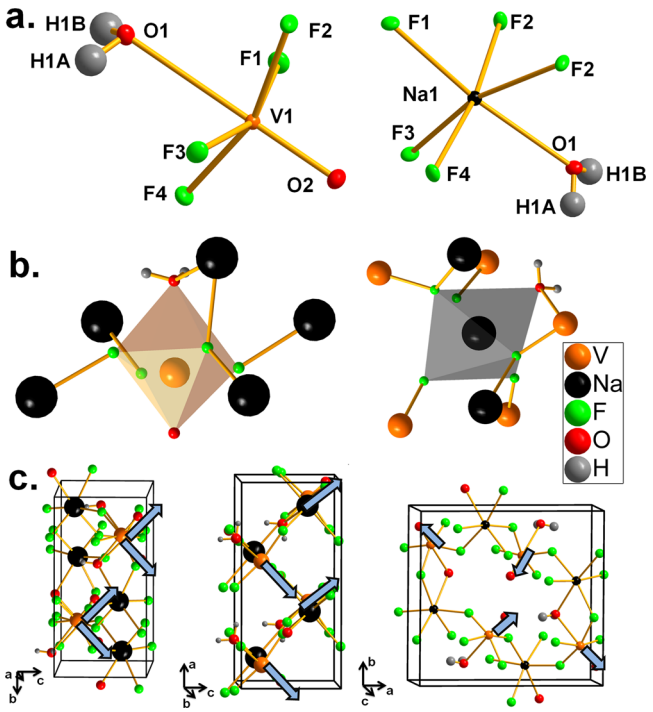

Figure 2. Representation of the structure of compound **I**. (a) Ordered, 0D anionic octahedra of $[VO_{1/1}F_{4/1}(H_2O)_{1/1}]^-$ and $[NaF_{2/2}F_{3/1}(H_2O)_{1/2}]^{3-}$. The fluoride and oxide anions and water moieties are ordered among the cations. The ellipsoids are drawn at the 50% probability level. (b) Coordination environment of the vanadium octahedral cation. (c) Views of the unit cell. The polar moments of the vanadium octahedral anions are shown with blue arrows; the polar moments are partially oriented along the *c* axis.

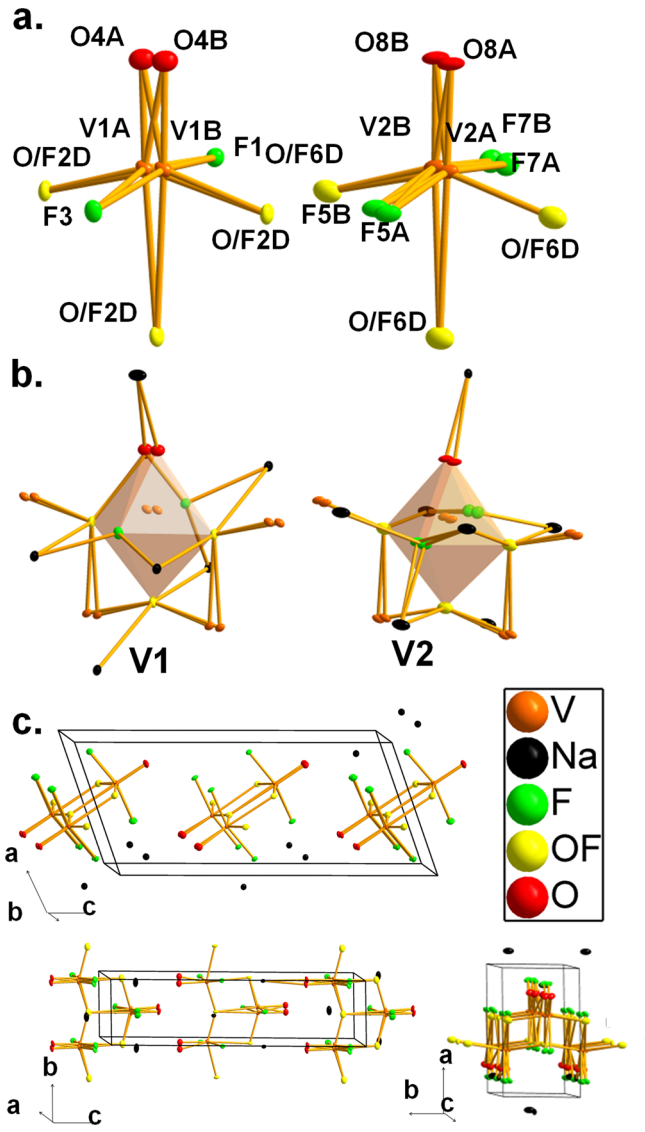

Figure 3. Representation of the structure of compound **II**. (a) Vanadium environments of V1 and V2. These sites are divided into two separate sites. The vanadium cations are disordered along the bonding axis of one symmetrically distinct anion; this anion is therefore disordered and was refined so as to account for the content of $NaVO_{2-x}F_{2+x}$ ($x = {}^1/_3$). (b) Environment of the polyhedra of V1 and V2. (c) Views of the unit cell.

unit cell of $NaVOF_4(H_2O)$ is shown in Figure 2c: the polar moments of the vanadium octahedra partially align along one axis (the polar *c* axis).

The structure of **II** is commensurately modulated and presents very interesting vanadium octahedra in 1D chains, namely, in the split sites of vanadium that are shown pictorially in Figure 3. The site occupancies show two vanadium sites in approximately 1:2 ratios, similar to the 1:2 vanadium(4+)/vanadium(5+) ratio of the chemical formula indicated by elemental analysis. The increase of the dimensionality (from 0D to 1D) for **I** and **II** is a result of increased temperature, which increases the condensation of vanadium oxide−fluoride BBUs.[44] General structure analysis of **II** is difficult in light of the disorder present, even under consideration of the supercell. The structure presents a total of four vanadium cation site positions. The vanadium cations are each disordered among two positions; the occupancies of these sites were refined so as to add to 1; this is consistent with the finding of the 1:1 sodium/vanadium ratio (it is *possible* that the sodium/vanadium ratio is 1:1 and the structure is equally sodium- and vanadium-deficient, but this is very unlikely). Free refinement of the sodium or vanadium cation occupancies in the crystallographic data resulted in full occupancy on each site. The vanadium sites are displaced along two bonds. This indicates that the anions along these bonds are disordered, mixed oxide−fluoride sites. The V−O bonds are typically shorter than the V−F bonds, and subsequently O/F disorder causes the ellipsoid of the anionic site to be elongated along the bonding axis. During refinement, this site was modeled as a disordered oxide−fluoride (2O:1F) site so as to maintain the formula found with elemental analyses.

Certain oxide and fluoride sites could be split and have their occupancies refined; these occupancies are relatively consistent with a parity of vanadium valence identity of 1:2 vanadium(4+)/vanadium(5+). The refined occupancies are displayed in the SI. The disordered vanadium octahedra are presented in Figure 3a.

There may be some correlation of the site occupancies with the 1:2 vanadium(4+)/vanadium(5+) ratio: the ions V1B, V2B, O4A, and F5A versus, respectively, V1A, V2A, O4B, and F5B refined in roughly 1:2−1:3 ratios. The individual octahedra of Figure 3a cannot be analyzed with bond-valence-sum calculations to determine if one site corresponds to vanadium(4+) or vanadium(5+) owing to the high degree of site identity and occupancy disorder. The representations of the environ-

dx.doi.org/10.1021/ic501486x | *Inorg. Chem.* 2015, 54, 765−772

ments of the vanadium anions are shown in Figure 3b. The unit cell of the structure is shown in Figure 3c.

SHG Responses of Compounds I and II. Both **I** and **II** have SHG responses on the same order of magnitude as α-SiO_2. These data may not be completely accurate owing to NaCl impurities present with **I** and absorptions of **II** in the near-IR (NIR) and visible regions. In the Kurtz−Perry experiment to examine SHG responses, the laser source (first harmonic) was 1064 nm and the measured output (second harmonic) was 532 nm. Compound **II** absorbs strongly in both regions (see the SI), so its SHG response is likely greater.

DISCUSSION

Elemental Content. ICP-AES and fluoride elemental analysis indicate the formula of compound **II** to be $Na(V^{4+}V^{5+}_2)_xO_{2-x}F_{2+x}$ where $x = {}^1/_3$. The crystallographic structure indicated disorder along bonds to two anions (see Figure 3c). The decreased cationic charge by reduction of vanadium(5+) to vanadium(4+) results in a decreased anionic charge by the partial replacement of oxygen(2−) with fluorine(1−). It is possible that a decreased anionic content is compensated for by oxide−fluoride site vacancies, but this is not observed in the single-crystal data: free refinement of the disordered anion as a fluoride ion results in a site occupancy of about 1, and refinement as an oxide site results in a site occupancy of about 1.1 (consistent with the presence of fluoride ions with a greater Z value than oxide ions).

Oxide−Fluoride Order in Compound I. Compound **I** is ordered in terms of oxide−fluoride anions or water molecules. Notably, the sodium ion packs in such a way that it predominantly coordinates to five fluoride anions and one water molecule; it does not coordinate to the softer oxide anion (softer relative to the fluoride anion). This is consistent with hard/soft acid/base interactions that have been previously observed and discussed.[9,23,24,45−49]

Mixed Valences of Compound II. The mixed valence of vanadium in **II** occurs on account of the presence of chloride ions in solution of hydrothermal synthesis. We infer that reduction occurs on account of generated hydrochloric acid (generated by chloride ions in highly acidic HF). Hydrochloric acid is a known reducing agent of vanadium(V).[25,26] When the reaction is performed with NaF as a sodium source in place of NaCl, a small amount of clear crystals are produced. The PXRD and single-crystal diffraction data show the crystals to have the same unit cell of **II**; that is, the clear material also shows a supercell (1 × 1 × 2) of $NaVO_2F_2$.[40] We were unable to reproduce the reported synthesis of $NaVO_2F_2$ because the synthesis required high temperatures (552 °C) with HF.

Mixed vanadate species generally have magnetic moments that correspond to noninteger numbers of electrons.[50−52] Thus, magnetic measurements showed **II** to have an effective magnetic moment of 0.303 μ_B/mol. The band gap was determined with UV−vis−NIR spectroscopy to be approximately 0.632 eV.

Mixed Valences in Previous Structures. Previous multivalent V_2O_5 materials have been reported in the literature. The mixed vanadium(4+)/vanadium(5+) valences occur in many compounds, and this property is of interest for battery and magnetic materials. However, mixed vanadium(3+)/vanadium(5+) valences are rare. These two species could be identified in previous structures owing to different environments: While vanadium(5+) cations may crystallize in a tetrahedral environment, vanadium(3+) cations do not. Thus, vanadium(3+) has been identified in the center of octahedra, while vanadium(5+) adopts a tetrahedral environment for $K_3V(VO_4)_2$,[53] and $Ba_3V_2O_3S_4$.[54] Other interesting structures such as $Ba_8V_7O_{22}$[55] and $Fe_{6.5}V_{11.5}O_{35}$[56] combine vanadium in three oxidation states: 3+, 4+, and 5+. These multivalent materials are usually identifiable by their distinct environment for the vanadium with different oxidation states. We conjecture, but cannot decisively prove, that the vanadium of **II** is present in the vanadium(4+) and vanadium(5+) states owing to the low magnetic moment and paramagnetic behavior at low temperatures. If vanadium(3+) ions were present, we could expect to observe inner-orbital interactions between the unpaired electrons of vanadium(3+). We do not observe tetrahedra in the crystal structure of **II**, so we are unable to decisively identify vanadium(5+) species. Bond-valence-sum calculations return noninteger values for the valence, indicating valence-site disorder.[57,58]

Polar Moment of Compound I. Compound **I** consists of discrete sodium octahedra and vanadium aqua−oxide−fluoride octahedra. The vanadium oxide−fluoride anions have a polar moment that is partially aligned along one axis (the polar c axis). The polar ions are separated by sodium ions into 0D BBUs (i.e., the vanadium octahedra do not share ions/water molecules with other vanadium octahedra). These sodium ions "shield" the polar moments of the overall structure from other polar moments; such an arrangement can be favorable because the polar moments do not have an adjacent neighbor. A vanadium BBU could situate itself antiparallel to a neighboring vanadium BBU to cancel out the polarity and maximize the local electroneutrality.[59]

The presence of such "mediating" ions that charge balance but still allow polar moments could be a viable path to develop NCS structures. This was found to be a factor in the polarity of the highly efficient SHG material $K_3B_6O_{10}Cl$; the potassium counterions contributed to the overall polarity of the structure.[8] In the structures of **I** and **II**, the sodium octahedra, via geometric calculations,[16] are found to be very weakly polar. From this analysis, the polar contribution to the SHG response of compounds **I** and **II** originates from the vanadium octahedra; however, more extensive density functional theory calculations should be performed to examine whether this is the case.[8] It should also be noted that, although the sodium cations are necessary for charge balance, they do "dilute" the polar contributions of individual ions in the structure. If the sodium ions could contribute to the polarity of the structure, a greater SHG response may be observed.[8]

In **I**, the vanadium polar moments pack in a 1D BBU of vanadium cations separated by a 1D ribbon of sodium cations. Figure 4a shows these coordination environments: the 2_1 screw axis of **I** describes the geometry of these ribbons, with oxide anions partially oriented in one direction. Figure 4b shows that these ribbons pack so that the terminal oxides of the vanadium BBUs are situated toward the channels. This type of environment minimizes the number of contacts to the terminal oxide; such an environment has been noted to correlate with NCS crystal classes;[9] however, this may be a correlation and not an inherent cause. The CS polymorph of $KNaNbOF_5$ only has one contact to the oxide: the linear Nb═O−K bond. It is likely that a reduced number of contacts to the terminal oxide of an ETM still *can* facilitate low-symmetry environments [such as in the NCS $KNaNbOF_5$ and $CuVOF_4(H_2O)_7$ systems].[60−62] These low coordination numbers avoid O_h and T_d environments around the oxide anion but do not necessarily avoid $C_{\infty v}$.

dx.doi.org/10.1021/ic501486x | Inorg. Chem. 2015, 54, 765−772

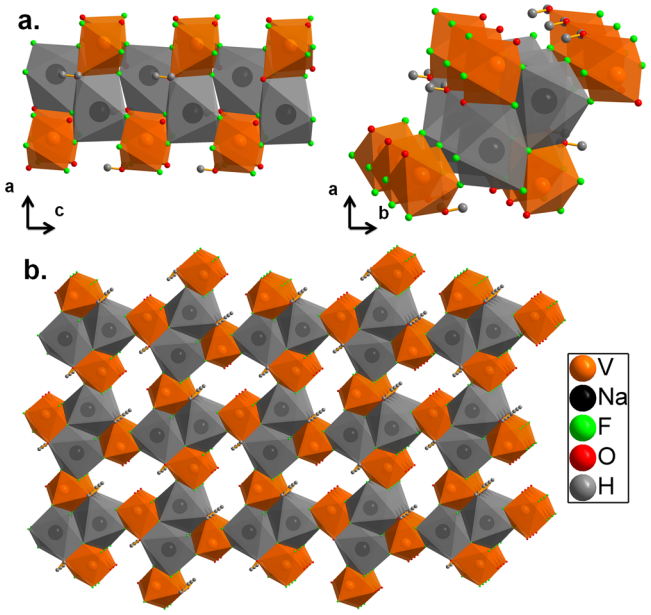

Figure 4. View of the compound **I** structure. (a) 1D unit of the individual vanadium oxide–fluoride BBUs as described by the 2_1 screw axis along the *c* axis. (b) Packing of the 1D units. Void space exists, and the terminal oxide anions are situated toward these voids.

This linear point group does not contain an inversion center but does allow a number of coordination environments: such variability can allow CS environments around the terminal oxide.

Polar Moments of Compound II. Initially, the structure of **II** looks nonpolar based on the unit cells shown in Figure 3. The disorder convolutes structural interpretation, but visualization of the structure of **II** in Figure 5 shows the preferential

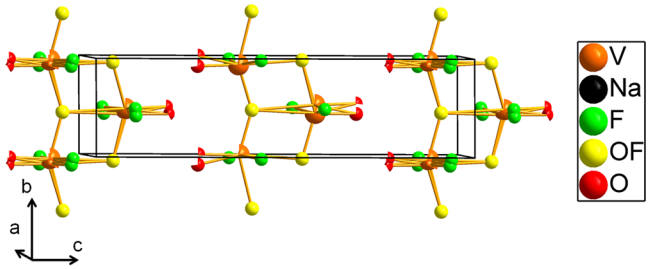

Figure 5. Partial occupancies illustrated with "pie chart" atoms: the unit cell of compound **II** with only the polyhedra of V2 shown. A polar moment exists along the *b* axis owing to the preference of one oxide anion to situate in one location; vanadium distortion is predominantly directed down the *b* axis.

presence of a terminal oxide and a vanadium ion in one location. The partial occupancies cause a vanadium cation to be situated "lower" (as viewed in Figure 5) within its octahedron along one axis. Traditionally, partial oxide–fluoride order is sought in systems to generate NCS materials.[47,58,60,63−68] This concept of partial disorder within an inorganic phase could allow (i) polar moments and (ii) stabilization afforded by increased entropy. This disorder could be introduced by in situ reduction/oxidation to modify known phases (such as, in this case, $NaVO_2F_2$).

Comparison to Previous Structures. Vanadium(5+) oxide is typified by a strong orange color.[26] Compound **I** is colorless owing to the presence of fluoride anions; these anions blue-shift the absorption of the metal into the UV region. This effect has been used in NCS materials of $K_2Be_2BO_3F_2$ and $Ba_4B_{11}O_{20}F$.[69,70] Such transparency in the UV region is necessary for SHG materials to provide high-energy lasers in the UV region for the potential use of lasers for nanolithography.[71]

The material $NaVOF_4{\cdot}0.7H_2O$ has been previously reported but not crystallographically described; the synthesis of the material is similar to the synthesis of **I**.[72] The structure of **I** is chemically and structurally similar to $[C_2N_2H_{10}][VOF_4(H_2O)]$.[73] Both structures contain 0D vanadium BBUs but differ in geometry. The zero dimensionality of the vanadium BBUs refers to coordination of the vanadium BBUs with other vanadium BBUs: each vanadium octahedron is isolated from other vanadium octahedra. The hybrid material of $[C_2N_2H_{10}][VOF_4(H_2O)]$ contains vanadium(4+) ions, while **II** contains vanadium(5+) ions. The former phase has greater polar alignment [at an angle of 25.241(63)° with respect to the polar *b* axis] compared to the latter phase [at an angle of 55.266(37)° with respect to the polar *b* axis]. The hybrid material's polar alignment is attributed to hydrogen bonds. Although hydrogen bonds are, in fact, present for **I**, the stronger interactions with the sodium ions are more influential within the phase. The SHG response of $[C_2N_2H_{10}][VOF_4(H_2O)]$ is about an order of magnitude greater than the SHG response of **I**. This may be a consequence of the presence of NaCl impurities within the sample of **I** but also may indicate a greater SHG response for $[C_2N_2H_{10}][VOF_4(H_2O)]$ on account of the polar alignment and Chen's Anionic Group Theory.[13]

Commensurate Structure of Compound II. As noted, **II** is a modulated variation of $NaVO_2F_2$.[39,40] The modulation is relatively complex to analyze because, from the solution of the supercell, the structure presents disorder in (i) the vanadium valence, (ii) vanadium site positions/occupancies, and (iii) oxide–fluoride positions/occupancies. The overall structure maintains the 1D BBU motif present in $NaVO_2F_2$. The FTIR spectrum of compound **II** shows numerous, broad peaks from 1020 to 500 cm^{-1}. The number and broadness indicates several (disordered) V=O and V–X (X = F^-, O^{2-}) bonding environments. The relatively high energy (1018 cm^{-1}) of one peak indicates that a strong V^{5+}=O bond is present.[9]

The single-crystal data do not indicate other long-range order to be present; e.g., there is no evidence of separate chains that consist of different geometries, nor are there signs of ordering of cations along the chain [such as every third vanadium in a chain being vanadium(4+)].

Phase Matchability of Compounds I and II. The two NCS compounds belong to different space groups but are chemically similar. The SHG responses obtained for **I** and **II** are about the same as that of $NaVO_2F_2$ (on the order of α-SiO_2).[40] Compound **II** absorbs strongly at the fundamental frequency that was used in the SHG measurement (1064 nm) and the second harmonic (532 nm) of light that was produced via SHG (see Figure 1). Therefore, the actual SHG efficiency of **II** is likely greater than that of $NaVO_2F_2$. Despite chemical similarity, **II** is PM and **I** is NPM. Phase matchability has been extensively described for organic molecular crystals;[74,75] future studies of inorganic systems are needed to rationalize the phase matchability in inorganic, extended solids.

dx.doi.org/10.1021/ic501486x | *Inorg. Chem.* 2015, 54, 765−772

CONCLUSION

The material $NaVOF_4(H_2O)$ is a 0D NCS material that was synthesized under reflux conditions. By increasing the synthetic temperature to hydrothermal conditions, the higher-dimensional (1D) material $NaVO_{2-x}F_{2+x}$ ($x = {}^1/_3$) was synthesized; it is a commensurately modulated variation of $NaVO_2F_2$. The modulated material is a multivalent compound that was obtained by in situ reduction with a "mild" reducing agent of NaCl in HF at 150 °C. Such materials could be of interest to multiferroics in addition to studies of SHG-active materials and fundamental solid-state synthetic chemistry. $NaVOF_4(H_2O)$ is type 1 NPM, while $NaVO_{2-x}F_{2+x}$ ($x = {}^1/_3$) is type 1 PM.

Future theoretical work into the effects of dispersion and electronic configurations of NCS materials should address the topic of phase matchability of extended, inorganic solids. An understanding of how materials may or may not be PM for industrial purposes would greatly enhance future targeted efforts to generate suitable materials for SHG purposes.

ASSOCIATED CONTENT

Supporting Information

Crystallographic data in CIF format, experimental details, and figures for single-crystal X-ray diffraction, PXRD, bond-valence-sum calculations, UV−vis−NIR spectroscopy, FTIR spectroscopy, and magnetism. This material is available free of charge via the Internet at http://pubs.acs.org.

AUTHOR INFORMATION

Corresponding Author

*E-mail: krp@northwestern.edu.

Author Contributions

The manuscript was written through contributions of all authors. All authors have given approval to the final version of the manuscript.

Notes

The authors declare no competing financial interest.

ACKNOWLEDGMENTS

This work was supported by funding from the National Science Foundation (Awards DMR-1005827 and DMR-1307698). We thank Charlotte Stern and Amy Sarjeant for helpful discussions regarding chemical structures. Single-crystal X-ray, ICP-AES, and FTIR data were acquired at Northwestern University's Integrated Molecular Structure Education and Research Center (IMSERC) at Northwestern University, which is supported by grants from NSF-NSEC, NSF-MRSEC, the KECK Foundation, the State of Illinois, and Northwestern University. P.S.H. and T.T.T. thank the Robert A. Welch Foundation (Grant E-1457) for support. PXRD data were collected at J. B. Cohen X-ray Diffraction Facility supported by the MRSEC program of the National Science Foundation (Grant DMR-1121262) in the Materials Research Center of Northwestern University. We gratefully acknowledge the assistance of Michael Graham and Professor Danna Freedman for magnetic measurements. These magnetic measurements were partially supported with funding from the International Institute for Nanotechnology and the State of Illinois DCEO Award 10-203031. Diffuse-reflectance UV−vis−NIR data were obtained at the Keck Biophysics Facility and Keck-II, which are supported by grants from the W. M. Keck Foundation, Northwestern University, the NIH, the Rice Foundation, and the Robert H. Lurie Comprehensive Cancer Center.

DEDICATION

Dedicated to the memory of John Corbett.

REFERENCES

(1) Miller, R. C. *Appl. Phys. Lett.* **1964**, *5*, 17.
(2) Rieckhoff, K. E.; Peticolas, W. L. *Science* **1965**, *147*, 610.
(3) Eaton, D. F. *Science (Washington, D.C.)* **1991**, *253*, 281.
(4) Halasyamani, P. S.; Poeppelmeier, K. R. *Chem. Mater.* **1998**, *10*, 2753.
(5) Chen, Q.; Chen, J. *Wuli* **1997**, *26*, 67.
(6) Chen, M.-C.; Li, L.-H.; Chen, Y.-B.; Chen, L. *J. Am. Chem. Soc.* **2011**, *133*, 4617.
(7) Norquist, A. J.; Heier, K. R.; Halasyamani, P. S.; Stern, C. L.; Poeppelmeier, K. R. *Inorg. Chem.* **2001**, *40*, 2015.
(8) Wu, H.; Pan, S.; Poeppelmeier, K. R.; Li, H.; Jia, D.; Chen, Z.; Fan, X.; Yang, Y.; Rondinelli, J. M.; Luo, H. *J. Am. Chem. Soc.* **2011**, *133*, 7786.
(9) Donakowski, M. D.; Gautier, R.; Yeon, J.; Moore, D. T.; Nino, J. C.; Halasyamani, P. S.; Poeppelmeier, K. R. *J. Am. Chem. Soc.* **2012**, *134*, 7679.
(10) Holland, M.; Donakowski, M. D.; Pozzi, E. A.; Rasmussen, A. M.; Tran, T. T.; Pease-Dodson, S. E.; Halasyamani, P. S.; Seideman, T.; Van Duyne, R. P.; Poeppelmeier, K. R. *Inorg. Chem.* **2013**, *53*, 221.
(11) Kanatzidis, M. G.; Poeppelmeier, K. R.; Bobev, S.; Guloy, A. M.; Hwu, S.-J.; Lachgar, A.; Latturner, S. E.; Schaak, E.; Seo, D.-K.; Sevov, S. C. *Prog. Solid State Chem.* **2008**, *36*, 1.
(12) Li, M.-R.; Stephens, P. W.; Retuerto, M.; Sarkar, T.; Grams, C. P.; Hemberger, J.; Croft, M. C.; Walker, D.; Greenblatt, M. *J. Am. Chem. Soc.* **2014**, *136*, 8508.
(13) Chen, C. T. *Acta Phys. Sin.* **1976**, *25*, 146.
(14) Kunz, M.; Brown, I. D. *J. Solid State Chem.* **1995**, *115*, 395.
(15) Agulyanskii, A. I.; Zavodnik, V. E.; Kuznetsov, V. Y.; Sidorov, N. V.; Stefanovich, S. Y.; Tsikaeva, D. V.; Kalinnikov, V. T. *Izv. Akad. Nauk SSSR, Neorg. Mater.* **1991**, *27*, 880.
(16) Maggard, P. A.; Nault, T. S.; Stern, C. L.; Poeppelmeier, K. R. *J. Solid State Chem.* **2003**, *175*, 27.
(17) Agulyanskii, A. I. *The Chemistry of Tantalum and Niobium Fluoride Compounds*; Elsevier: Amsterdam, The Netherlands, 2004.
(18) Bera, T. K.; Jang, J. I.; Ketterson, J. B.; Kanatzidis, M. G. *J. Am. Chem. Soc.* **2008**, *131*, 75.
(19) Gautier, R.; Poeppelmeier, K. R. *Cryst. Growth Des.* **2013**, *13*, 4084.
(20) Maggard, P. A.; Nault, T. S.; Stern, C. L.; Poeppelmeier, K. R. *J. Solid State Chem.* **2003**, *175*, 27.
(21) Ok, K. M.; Halasyamani, P. S.; Casanova, D.; Llunell, M.; Alemany, P.; Alvarez, S. *Chem. Mater.* **2006**, *18*, 3176.
(22) Mun, E. D.; Chern, G.-W.; Pardo, V.; Rivadulla, F.; Sinclair, R.; Zhou, H. D.; Zapf, V. S.; Batista, C. D. *Phys. Rev. Lett.* **2014**, *112*, 017207.
(23) Donakowski, M. D.; Vinokur, A. I.; Poeppelmeier, K. R. *Z. Anorg. Allg. Chem.* **2012**, *638*, 1991.
(24) Donakowski, M. D.; Görne, A.; Vaughey, J. T.; Poeppelmeier, K. R. *J. Am. Chem. Soc.* **2013**, *135*, 9898.
(25) Foster, H. B. U.S. Patent 2,180,353, 1933; p 1.
(26) Cotton, F. A.; Wilkinson, G.; Murillo, C. A.; Bochmann, M. *Advanced Inorganic Chemistry*, 6th ed.; John Wiley & Sons, Inc.: New York, 1999; p 718.
(27) Donakowski, M. D.; Lu, H.; Gautier, R.; Saha, R.; Sundaresan, A.; Poeppelmeier, K. R. *Z. Anorg. Allg. Chem.* **2014**, *640*, 1109.
(28) Bertolini, J. C. *J. Emerg. Med.* **1991**, *10*, 163.
(29) Peters, D.; Miethchen, R. *J. Fluorine Chem.* **1996**, *79*, 161.
(30) Segal, E. B. *Chem. Health Saf.* **2000**, *7*, 18.
(31) Leuschner, J.; Haschke, H.; Sturm, G. *Monatsh. Chem.* **1994**, *125*, 623.
(32) Harrison, W. T. A.; Nenoff, T. M.; Gier, T. E.; Stucky, G. D. *Inorg. Chem.* **1993**, *32*, 2437.
(33) Norquist, A. J.; Heier, K. R.; Stern, C. L.; Poeppelmeier, K. R. *Inorg. Chem.* **1998**, *37*, 6495.

(34) Halasyamani, P. S.; Heier, K. R.; Norquist, A. J.; Stern, C. L.; Poeppelmeier, K. R. *Inorg. Chem.* **1998**, *37*, 369.
(35) *SAINT*, 7.23A ed.; Bruker Analytical X-ray Instruments, Inc.: Madison, WI, 2005.
(36) Sheldrick, G. *APEX2*; University of Göttingen: Göttingen, Germany, 1996.
(37) Sheldrick, G. *Acta Crystallogr., Sect. A* **2008**, *64*, 112.
(38) Dolomanov, O. V.; Bourhis, L. J.; Gildea, R. J.; Howard, J. A. K.; Puschmann, H. J. *Appl. Crystallogr.* **2009**, *42*, 339.
(39) Sengupta, A. K.; Bhaumik, B. B. *Z. Anorg. Allg. Chem.* **1971**, *384*, 255.
(40) Crosnier-Lopez, M. P.; Duroy, H.; Fourquet, J. L.; Abrabri, M. *Eur. J. Solid State Inorg. Chem.* **1994**, *31*, 957.
(41) Hamilton, W. *Acta Crystallogr.* **1965**, *18*, 502.
(42) Spek, A. L. *PLATON*; Utrecht University: Utrecht, The Netherlands, 2001.
(43) Kurtz, S. K.; Perry, T. T. *J. Appl. Phys.* **1968**, *39*, 3798.
(44) Aldous, D. W.; Stephens, N. F.; Lightfoot, P. *Dalton Trans.* **2007**, 4207.
(45) Pearson, R. G. *Chemical Hardness*; John Wiley & Sons, Inc.: New York, 1997.
(46) Shannon, R. D.; Fischer, R. X. *Phys. Rev. B* **2006**, *73*, 235111.
(47) Marvel, M. R.; Pinlac, R. A. F.; Lesage, J.; Stern, C. L.; Poeppelmeier, K. R. *Z. Anorg. Allg. Chem.* **2009**, *635*, 869.
(48) Aldous, D. W.; Lightfoot, P. *Solid State Sci.* **2009**, *11*, 315.
(49) Fry, A. M.; Seibel, H. A.; Lokuhewa, I. N.; Woodward, P. M. *J. Am. Chem. Soc.* **2011**, *134*, 2621.
(50) Baxter, S. M.; Wolczanski, P. T. *Inorg. Chem.* **1989**, *28*, 3263.
(51) Das, S.; Niazi, A.; Mudryk, Y.; Pecharsky, V. K.; Johnston, D. C. *Phys. Rev. B* **2010**, *81*, 104432.
(52) Keene, T. D.; D'Alessandro, D. M.; Krämer, K. W.; Price, J. R.; Price, D. J.; Decurtins, S.; Kepert, C. J. *Inorg. Chem.* **2012**, *51*, 9192.
(53) Abriel, W.; Rau, F.; Range, K. J. *Mater. Res. Bull.* **1980**, *15*, 1099.
(54) Calvagna, F.; Zhang, J.; Li, S.; Zheng, C. *Chem. Mater.* **2001**, *13*, 304.
(55) Liu, G.; Greedan, J. E. *J. Solid State Chem.* **1994**, *108*, 371.
(56) Grey, I. E.; Anne, M.; Collomb, A.; Muller, J.; Marezio, M. *J. Solid State Chem.* **1981**, *37*, 219.
(57) Brown, I. D. *Phys. Chem. Miner.* **1987**, *15*, 30.
(58) Chamberlain, J. M.; Albrecht, T. A.; Lesage, J.; Sauvage, F. d. r.; Stern, C. L.; Poeppelmeier, K. R. *Cryst. Growth Des.* **2010**, *10*, 4868.
(59) Pauling, L. *J. Am. Chem. Soc.* **1929**, *51*, 1010.
(60) Marvel, M. R.; Lesage, J.; Baek, J.; Halasyamani, P. S.; Stern, C. L.; Poeppelmeier, K. R. *J. Am. Chem. Soc.* **2007**, *129*, 13963.
(61) Pinlac, R. A. F.; Stern, C. L.; Poeppelmeier, K. R. *Crystals* **2011**, *1*, 3.
(62) Vasiliev, A. D.; Laptash, N. M. *J. Struct. Chem.* **2012**, *53*, 902.
(63) Welk, M. E.; Norquist, A. J.; Stern, C. L.; Poeppelmeier, K. R. *Inorg. Chem.* **2000**, *39*, 3946.
(64) Welk, M. E.; Norquist, A. J.; Arnold, F. P.; Stern, C. L.; Poeppelmeier, K. R. *Inorg. Chem.* **2002**, *41*, 5119.
(65) Izumi, H. K.; Kirsch, J. E.; Stern, C. L.; Poeppelmeier, K. R. *Inorg. Chem.* **2005**, *44*, 884.
(66) Gautier, R.; Donakowski, M. D.; Poeppelmeier, K. R. *J. Solid State Chem.* **2012**, *195*, 132.
(67) Lu, H.; Gautier, R.; Donakowski, M. D.; Tran, T. T.; Edwards, B. W.; Nino, J. C.; Halasyamani, P. S.; Liu, Z.; Poeppelmeier, K. R. *J. Am. Chem. Soc.* **2013**, *135*, 11942.
(68) Fry, A. M.; Woodward, P. M. *Cryst. Growth Des.* **2013**, *13*, 5404.
(69) Wu, B.; Tang, D.; Ye, N.; Chen, C. *Opt. Mater. (Amsterdam)* **1996**, *5*, 105.
(70) Wu, H.; Yu, H.; Yang, Z.; Hou, X.; Su, X.; Pan, S.; Poeppelmeier, K. R.; Rondinelli, J. M. *J. Am. Chem. Soc.* **2013**, *135*, 4215.
(71) Nowak, K. M.; Ohta, T.; Suganuma, T.; Fujimoto, J.; Mizoguchi, H.; Sumitani, A.; Endo, A. *Opto-Electron. Rev.* **2013**, *21*, 345.
(72) Sengupta, A. K.; Bhaumik, B. B. *Z. Anorg. Allg. Chem.* **1971**, *384*, 251.
(73) Stephens, N. F.; Buck, M.; Lightfoot, P. *J. Mater. Chem.* **2005**, *15*, 4298.
(74) Zyss, J.; Oudar, J. L. *Phys. Rev. A* **1982**, *26*, 2028.
(75) Yamamoto, H.; Katogi, S.; Watanabe, T.; Sato, H.; Miyata, S.; Hosomi, T. *Appl. Phys. Lett.* **1992**, *60*, 935.